Polymer/Metal Oxide Nanocrystals Hybrid Solar Cells

Shao-Sian Li, Yun-Yue Lin, Wei-Fang Su, and Chun-Wei Chen

Abstract—**In this paper, we present two different types of polymer/metal oxide nanocrystals hybrid photovoltaics. One is the poly(3-hexylthiophene) (P3HT)/TiO_2 nanorods hybrid bulk heterojunction (BHJ) solar cell and the other is a nanostructured ZnO/P3HT hybrid solar cell. In a BHJ hybrid solar cell, the dispersed semiconducting nanocrystals lead to an increased interface area between polymer and nanocrystals, which can assist charge separation for photogenerated carriers, but at the expense of poorly formed conducting pathways for electron transport. In contrast, a nanostructured hybrid solar cell usually consists of rigidly connected nanocrystals, which can provide direct pathways for electron transport, but the interface area between polymer and nanocrystals is limited. We have demonstrated that through interface modification with effective molecules, the photovoltaic performance in both device structures can be largely improved by enhancing charge separation and suppressing interface recombination rate in the polymer/inorganic hybrids.**

Index Terms—**Bulk heterojunction (BHJ), nanostructured solar cell, organic/inorganic hybrid, polymer solar cells.**

I. INTRODUCTION

O VER THE past decade, polymer solar cells have been the objects of interest in developing low-cost, large-area, and mechanically flexible photovoltaic devices [1], [2]. Because of the low dielectric constant of these molecular semiconductors, the photoexcitation generated coulomb-bound electron-hole pairs (excitons) rather than free electrons and holes. An internal field difference created by second phase of acceptor materials is usually needed for exciton to dissociate into free carriers. Until now, a promising power conversion efficiency of 4%–5% is based on poly(3-hexylthiophene) (P3HT)/fullerene derivatives bulk heterojunctions (BHJs) [2], [3], which consists of an electron-accepting network formed randomly within polymer matrix (donor). An alternative type of polymer solar cell including polymer/inorganic nanocrystal hybrid is also appealing because of relatively high electron mobility and good physical and chemical stability of inorganic nanocrystals [4]. Various nanocrystals such as CdSe [1], [5], PbS [6], TiO_2 [7]–[11], and ZnO [12] have been successfully used in polymer/inorganic nanocrystal hybrid solar cells. The replacement of toxic pre-
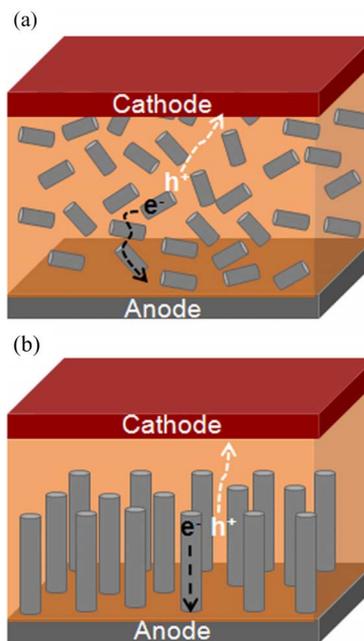
Fig. 1. Demonstration of two different constructions of polymer solar cells. (a) BHJ solar cell. (b) Nanostructured solar cell. Carrier transport paths were indicated by dashed arrows. Hole transport through polymer phase and electron hop through TiO_2 network pathways in BHJs or directly pass along ZnO nanorods in nanostructured solar cells.

cursors, such as Cd, Pb, by environmentally friendly metal oxides has also received similar interest. Two most common device structures have been proposed to fabricate the polymer/inorganic nanocrystal hybrid solar cells: 1) by blending dispersed nanocrystals within polymer to form BHJs [8], [10], [11]; or 2) by infiltrating polymer into rigid and well-connected nanoporous or nanorod structures [7], [9] to form nanostructured hybrid solar cells. In a BHJ hybrid solar cell, the dispersed semiconducting nanocrystals usually have a smaller size, which increase the interface area between polymer and nanocrystals, thereby assisting charge separation for photogenerated carriers, but at the expense of poorly formed conducting pathways for electron transport. In contrast, a nanostructured hybrid solar cell usually consists of rigidly connected nanocrystals, which can provide direct pathways for electron transport; however, the interface area between polymer and nanocrystals is limited by the larger dimension of the nanostructures. In this paper, we would like to present the polymer/inorganic nanocrystal hybrid solar cells consisting of two different device structures based on the P3HT/TiO_2 nanorods BHJs and nanostructured ZnO/P3HT hybrids, as shown in Fig. 1(a) and (b), respectively.
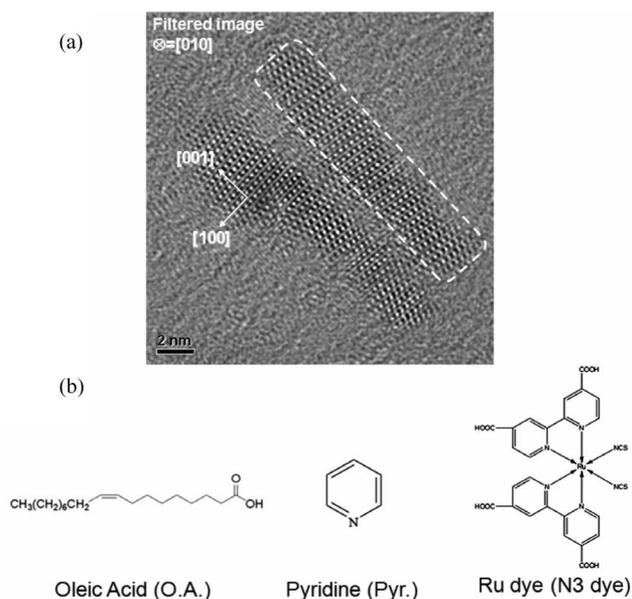
Fig. 2. HRTEM image of TiO$_2$ nanorods used in this paper. TiO$_2$ nanorods were capped by OA originally, but were replaced by Pyr and N3 dye in the following process.

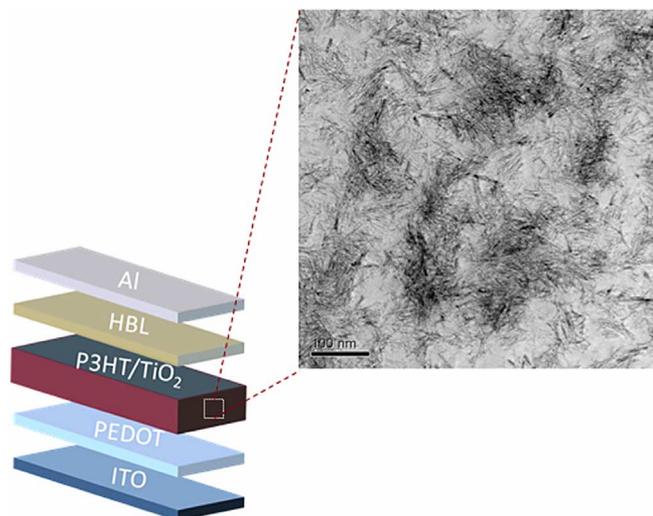
Fig. 3. Structure of a complete BHJ solar cell device including ITO as anode, PEDOT:PSS as hole transport layer, active layer consist of P3HT/TiO$_2$ hybrids, thin TiO$_2$ layer as hole-blocking layer, and Al as cathode. Also shown is TEM image of P3HT/TiO$_2$ nanorods hybrids.

II. POLYMER/TiO$_2$ BHJ SOLAR CELLS

A. Preparation of Materials

The high aspect ratio anatase titanium dioxide (TiO$_2$) nanorods were synthesized via hydrolysis of titanium tetraiso-propoxide, according to the literature with modification [13]. Details and results have been described in an earlier work [14]. TiO$_2$ nanorods have a dimension of 20–40 nm in length and 4–5 nm in diameter, as was revealed by the high-resolution transmission electron microscopy (HRTEM) image in Fig. 2(a). Typically, the as-synthesized TiO$_2$ nanorods are capped with insulating surfactant of oleic acid (OA) consisting of a long alkyl chain, which may act as a potential barrier for charge transfer. We, therefore, carried out the interface modification to replace the original OA ligand using two different kinds of ligand molecules, i.e., pyridine (Pyr) and cis–bis(4,4-dicarboxy-2,2-bipyridine) dithiocyanato ruthenium(II) (N3 dye), respectively. The three different kinds of surface ligands are shown schematically in Fig. 2(b).

Ligand replacement processes are as follows. First, the as-synthesized OA end-capped TiO$_2$ nanorods were washed three times with ethanol to remove the OA. Then, the TiO$_2$ nanorods were dispersed in Pyr and left under stirring at 70 °C until the solution turned clear. Through these procedures, the OA (original surface ligand) was removed and the Pyr of a weak-binding ligand was on the surface of TiO$_2$ nanorods. To obtain the N3 dye-modified TiO$_2$ nanorods, the as-synthesized OA-capped TiO$_2$ nanorods were mixed with the dyes in an approximate 500:1 weight ratio, dispersed in pyridine, and left stirred at 75 °C until the solution turned clear and purple, which is the color of N3 dye. The ligand molecule of N3 dye, consisting of carboxylate groups –COOH, can be attached strongly to TiO$_2$ nanorod surface.

B. Device Fabrication

For the photovoltaic device fabrication, a 40-nm thick layer of poly(3,4-ethylenedioxythiophene) (PEDOT):poly(styrenesulfonate (PSS) (Baytron P 4083) was spin cast onto the precleaned indium tin oxide (ITO) substrate, followed by baking at 120 °C for 30 min before moving into a nitrogen-purged glove box for subsequent depositions. The P3HT:TiO$_2$ nanorods hybrid was composed of a 1:1 weight ratio of P3HT ($M_w \sim 58000$, polydispersity index (PDI) 1.62, Regioregularity (RR) 96%) to TiO$_2$ in 10 mg/ml solution with the mixed solvent including pyridine, chloroform, dichloromethane, and chlorobenzene. After the P3HT/TiO$_2$ active layer was deposited by spin coating, the resulting thickness was about 120 nm. The Al electrode was deposited by thermal evaporation in a vacuum, under pressure of around 2×10^{-6} torr. The device's area was defined to be about 0.1 cm^2. A very thin layer of TiO$_2$ nanorods was sandwiched between the active layer and the aluminum electrode to act as a hole-blocking layer [14] as well as an optical spacer [15]. Fig. 3 shows structural schematics of a complete BHJ device and TEM images of this hybrid material as well. From the TEM image of P3HT/TiO$_2$ hybrids, we can observe that TiO$_2$ nanorods were well dispersed in P3HT matrix, forming a complex network for electron transport.

UV-Visible absorption spectra were obtained using Jasco V-570 UV/Vis/NIR Spectrophotometer. The steady-state photoluminescence (PL) spectra were taken by the FluoroLog-3 spectrofluorometer (HORIBA Jobin Yvon). Time-resolved photoluminescence (TRPL) spectroscopy was performed with a time-correlated single photon counting spectrometer (Picoquant, Inc.). A pulse laser (470 nm) with an average power of 1 mW operating at 40 MHz with duration of 70 ps was used for excitation. I–V measurements (Keithley 2410 source meter) were obtained by using a solar simulator (Newport Inc.) with the air mass (AM) 1.5 filter under irradiation intensity of
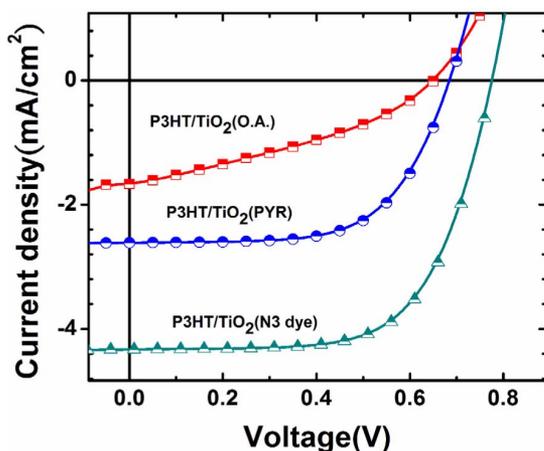
Fig. 4. *I–V* characteristics of P3HT/TiO$_2$ BHJ solar cells using different interface ligand molecules under AM 1.5 (100 mW/cm^2) irradiation.

100 mW/cm^2. The film thickness was measured by means of the Veeco M6 surface profiler.

C. Results and Discussion

The *I–V* characteristics of the devices with different configurations under simulated AM 1.5 illumination are shown in Fig. 4. The device based on the P3HT:TiO$_2$ nanorods (OA) hybrid material exhibits a short-circuit current density (J_{sc}) of 1.67 mA/cm^2, an open-circuit voltage (V_{oc}) of 0.65 V, and a fill factor (FF) of 0.35, resulting in a power conversion efficiency (η) of 0.38%. For the device based on the hybrid with TiO$_2$ nanorods by pyridine treatment, a large increase in the FF indicates that removal of insulating surfactant on the TiO$_2$ nanorods results in a significant improvement in the serial resistance of the device. The performance of the device based on the P3HT:TiO$_2$ nanorods (PYR) hybrid material exhibits a short-circuit current density (J_{sc}) of 2.61 mA/cm^2, an open-circuit voltage (V_{oc}) of 0.69 V, and a FF of 0.62, resulting in a η of 1.12%. For the device consisting of TiO$_2$ nanorods modified by the N3 dye molecule, a further improvement in the device performance is found, giving a short-circuit current density (J_{sc}) of 4.33 mA/cm^2, an open-circuit voltage (V_{oc}) of 0.78 V, and a FF of 0.65, resulting in a η of 2.20%. It is worth noting that the amount of adsorbed N3 dye on TiO$_2$ nanorod surface is estimated to be low about 1.3×10^{-12} mole/cm^2 of TiO$_2$ nanorod [16] and a negligible optical density of interface layers of these molecules in relation to that of P3HT was also found. This result indicates that these ligand molecules modify the interface rather than harvest light.

The interfacial molecules can 1) facilitate charge separation; or 2) prevent back recombination at the interfaces of P3HT/TiO$_2$ nanorod hybrids. TRPL and transient open-circuit voltage decay (TOCVD) measurements were performed to examine the two types of carrier dynamics in hybrids after interface modification. Fig. 5(a) shows the PL of P3HT/TiO$_2$ hybrids and suggests the occurrence of PL quenching from charge separation. The PL quenching efficiency Q for the three samples is $Q_{N3} > Q_{Pyr} > Q_{OA}$, which indicates that more efficient charge separation can be achieved at the P3HT/TiO$_2$ nanorods
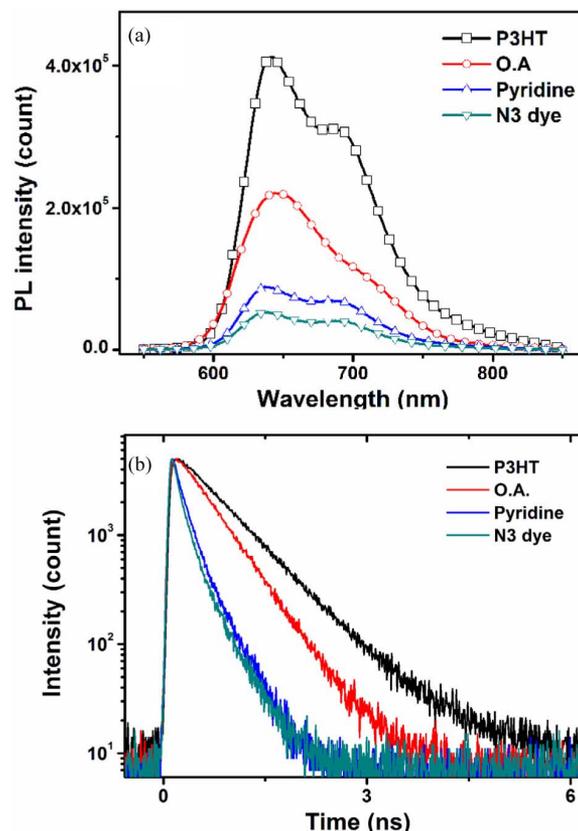

Fig. 5. (a) PL spectrum and (b) TRPL spectroscopy of P3HT/TiO$_2$ nanorod hybrids following different interface modifications.

interfaces by either removing the insulating surfactant or replacing it with a more conductive ligand. The improved charge separation efficiency at the P3HT/TiO$_2$ nanorods interfaces can also be inferred from TRPL spectroscopy. Fig. 5(b) shows the PL decay curves for the pristine P3HT and the hybrid films with different surface modification, respectively. The addition of TiO$_2$ nanorods in polymer results in a new relaxation process that provides a further nonradiative process to the donor, and leads to shortening of the measured lifetime τ. The measured PL lifetime for the pristine P3HT and P3HT/TiO$_2$ nanorods hybrid with OA, PYR, and N3 surfactant are $\tau_{P3HT} = 676$ ps, $\tau_{OA} = 480$ ps, $\tau_{PYR} = 255$ ps, and $\tau_{N3} = 232$ ps, respectively, indicating that more efficient charge separation takes place at the polymer/TiO$_2$ nanorods interfaces by removing the insulating ligand OA or replacing with a more conductive ligand of Pyr and N3 dye, consistent with the PL quenching result.

However, the effect of enhanced charge separation efficiency alone cannot account for the significant improvement in both J_{sc} and V_{oc} of the devices upon interface modification. Accordingly, TOCVD measurements were performed to determine the recombination rate at the interfaces between polymer and TiO$_2$ nanorods in an operating solar cell device under an open-circuit condition. A small perturbation generated by a pulsed laser produces extra electrons and holes in hybrids. The decay of the photovoltage that is generated by the additional carriers from the small perturbation corresponds to the recombination rate at
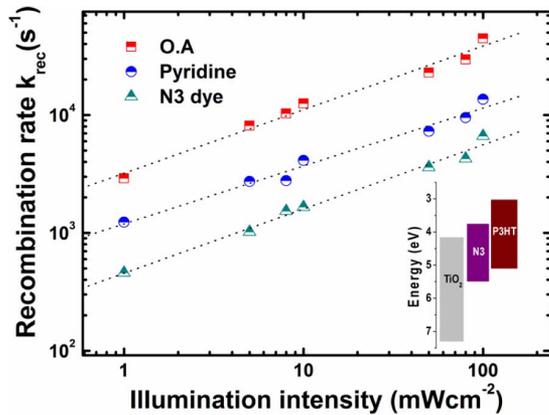
Fig. 6.   Charge recombination rate constant k_{rec} versus light intensity at open-circuit voltage determined by TOCVD measurement. Inset is the relative energy position of N3 dye in P3HT/TiO$_2$ BHJ solar cells.

the heterojunctions. Fig. 6 plots the charge recombination rate constant k_{rec} versus illumination intensity under open-circuit conditions. The recombination rates k_{rec} follow the order OA capped sample > pyridine modified sample > N3 dye modified samples at all light intensities, showing a good consistence with the photovoltaic performance. The interface modifier of the N3 dye molecule acts as the most effective recombination barrier with respect to other ligand molecules. As described earlier, the reduced recombination rate may lead to increased electron and hole concentrations at interfaces, increasing the difference between the quasi-Fermi levels of electrons and holes, and accounting for the observed increase in V_{oc} upon interface modifications. Furthermore, the suppression of back recombination at the interfaces can increase the number of carriers that can be transported toward electrodes, as a result of improved J_{sc} after interface modification. From the aforementioned result, it is concluded that interface modifications on the TiO$_2$ nanorod surface can be used to improve the performance of the device significantly by enhancing charge separation, while strongly suppressing back recombination, which take place at P3HT and TiO$_2$ heterojunctions.

III. NANOSTRUCTURED ZnO/POLYMER HYBRID SOLAR CELLS

Another type of polymer/metal oxide hybrid photovoltaic device is based on nanostructured ZnO/polymer hybrid solar cells, which can provide direct electron pathways as shown in Fig. 1. Here, we further propose a hybrid nanostructured polymer solar cell by providing more interface for exciton dissociation based on the ZnO/P3HT:TiO$_2$ hybrid material, as represented in Fig. 7(c). Thicker ZnO nanorod arrays are grown on the electrode surface to provide direct pathways for efficient electron collection. The thinner TiO$_2$ nanorods are then incorporated into polymer to provide larger interfacial areas and more effective conduction paths for charge separation and transport, respectively.

ZnO nanorod arrays were grown on ITO substrates covered with a layer of very thin gold nanocrystal as catalyst and using a low-temperature pulsed current electrolysis method, as de-
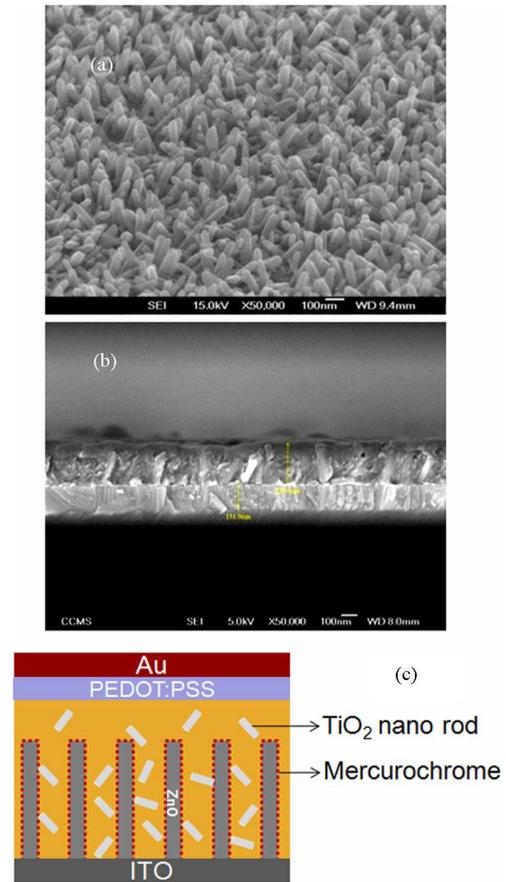

Fig. 7.   SEM image of (a) ZnO nanorods grown by low-temperature process and (b) cross section after infiltration of polymer. (c) Structural schematics of ZnO:mer/(P3HT/TiO$_2$) device.

scribed earlier [17]. Fig. 7(a) shows the typical scanning electron microscopy (SEM) image of the ZnO nanorod array. The ZnO nanorod array exhibits an average diameter of $\sim$50 nm and an average length of $\sim$180 nm [17], [18]. P3HT/TiO$_2$ nanorods hybrid was then spin cast onto ZnO nanorods substrate, and Fig. 7(b) shows the cross-sectional SEM image after the infiltration of the P3HT:TiO$_2$ nanorods hybrid. The thin active layer with a thickness of 200 nm was used as light absorbing and hole transporting material. The device was then followed by spin coating a layer of PEDOT:PSS as a buffer layer and a hole-transport layer with an effective thickness of 50 nm before thermal evaporation of the Au top electrode. The films were then baked in a vacuum oven for 6 h at 120 °C. Vapor deposition of the Au top electrode was then carried out at a pressure around 2×10^{-6} torr.

Moreover, we had demonstrated that the interfacial recombination can be suppressed by using effective ligand molecules between polymer and inorganic nanocrystals in the above results. We, therefore, used the organic molecule of mercurochrome (C$_{20}$H$_8$Br$_2$HgNa$_2$O) as the interface modifier, which is one of the best photosensitizer for ZnO photoanode [19] to date and is much cheaper than the Ru-complex dyes (N3 dye). The dip-coating process was carried out before polymer infiltration and the optical density of adsorbed dye on the ZnO surface was

TABLE I
DEVICE PERFORMANCE OF ZnO/P3HT AND ZnO/(P3HT/TiO₂) HYBRID
SOLAR CELLS BEFORE AND AFTER INTERFACE MODIFICATION

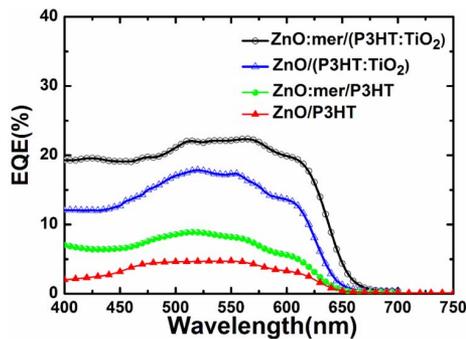|	Jsc (mA/cm2)	Voc (V)	FF (%)	η (%)
ZnO/P3HT	0.30	0.34	40	0.04
ZnO:mer/P3HT	0.87	0.45	41	0.16
ZnO/ (P3HT:TiO₂)	1.96	0.38	40	0.30
ZnO:mer/ (P3HT/TiO₂)	2.45	0.46	46	0.52

Fig. 8. External quantum efficiencies of ZnO/P3HT hybrid solar cell based on four different architectural structures.

negligible compared to that of the active layer's, indicating that photogenerated carriers were mainly from the active layer rather than from mercurochrome [18].

Results of the *I–V* characteristics of the devices based on the nanostructured ZnO/P3HT and nanostructured ZnO/P3HT:TiO₂ hybrid had been published in [16] and [17], and the overall device performance is summarized in Table I. After interface modification by attaching mercurochrome molecules on ZnO nanorod surface, both short-circuit current (J_{sc}) and open-circuit voltage (V_{oc}) of the ZnO/P3HT hybrid devices can be largely improved. In addition, due to a short exciton diffusion length of polymer (<20 nm) [20] with respect to an average spacing between nanorods of ∼100 nm, as reported previously, we have further incorporated thinner TiO₂ nanorods synthesized as described above into P3HT to increase the number of interfaces for charge separation. Not only the exciton lifetime decreased but also the device responding time reduced as well [17], indicating that an effective transport can be achieved by this hybrid architectural design. We have also compared the performance of nanostructured ZnO/P3HT:TiO₂ nanorod hybrid solar cells before and after interface modification as shown in Table I. A large improvement in both short circuit current (J_{sc}) and open-circuit voltage (V_{oc}) can also be obtained after interface modification on ZnO nanorod surface. The corresponding external quantum efficiencies of these devices are shown in Fig. 8. The result indicates that the organic photovoltaic performance based on this nanoctructured hybrid materials can be largely improved by simply incorporating thinner TiO₂ nanorods into active layer

and by modifying the ZnO/P3HT interfaces with effective ligand molecules of mercurochrome.

Devices with ZnO/P3HT:TiO₂ architecture, as shown in Fig. 7(c) provide efficient conduction pathways for electron to be collected by bottom electrode along vertically standing ZnO nanorods, but yet resulted in a relatively lower solar cell performance compared to P3HT/TiO₂ BHJ solar cells. Large dimensional ZnO nanostructure limited interface area between polymer/inorganic nanocrystals and incurred inefficient charge separation [17], [18]. The incorporation of thinner TiO₂ nanorods into P3HT/ZnO hybrid could not only highly increase the interface area but also formed a tradeoff between number of interface area and amount of leakage current. This leakage current could come from the percolation of TiO₂ nanocrystals and ZnO nanorods at high TiO₂ concentration. For further improvement of polymer/nanostructured ZnO hybrid solar cells, size, orientation, and spacing of ZnO nanorods must be studied.

We have further carried out the TOCVD to investigate the influence of interface modifier on the recombination rate at ZnO nanorods/P3HT interfaces. The recombination rate k_{rec} is, therefore, proportional to $1/\tau$ where τ is the decay lifetime of the transient photovoltage. It shows the photovoltage decay curves of devices based on ZnO/P3HT:TiO₂ nanorod hybrid, before and after interface modification. The recombination rate k_{rec} for the two devices are 1.2×10^4 s⁻¹ (before modification) and 4.5×10^3 s⁻¹ (after modification), respectively [18]. The result indicates that the interfacial layer can effectively prevent from back recombination at P3HT/ZnO interfaces. The reduced recombination rate may lead to increased electrons and holes concentrations at interfaces. As a result, the difference between the quasi-Fermi levels of electrons and holes will be increased, which can account for the observed increased V_{oc} after interface modifications. The aforementioned result suggests that the interface modifier of mercurochrome molecules attached on ZnO nanorod surface can also play an important role in assisting charge separation and preventing from back recombination at interfaces.

IV. CONCLUSION

In summary, we have fabricated polymer/inorganic nanocrystals hybrid solar cells with two types of structure: 1) P3HT/TiO₂ nanorods BHJ solar cell; and 2) nanostructured ZnO/P3HT hybrid solar cell. The device performance is largely dependent on nanomorphology of polymer/nanocrystal hybrid. In addition, by interface modification with effective molecules, the photovoltaic performance in both device structures can be largely improved due to enhanced charge separation and suppressed interface recombination rate in the polymer/inorganic hybrids. Our result provides a new route for future low-cost, environmentally friendly, photovoltaic applications.

Center for Condensed Matter Science, Taiwan, for high resolution TEM and SEM support.

REFERENCES

[1] W. U. Huynh, J. J. Dittmer, and A. P. Alivisatos, "Hybrid nanorod-polymer solar cells," *Science*, vol. 295, pp. 2425–2427, 2010.

[2] W. Ma, C. Yang, X. Gong, K. Lee, and A. J. Heeger, "Thermally stable, efficient polymer solar cells with nanoscale control of the interpenetrating network morphology," *Adv. Funct. Mater.*, vol. 15, pp. 1617–1622, 2005.

[3] G. Li, V. Shrotriya, J. Huang, Y. Yao, T. Moriarty, K. Emery, and Y. Yang, "High-efficiency solution processable polymer photovoltaic cells by self-organization of polymer blends," *Nat. Mater.*, vol. 4, pp. 864–868, 2005.

[4] J. Bouclé, P. Ravirajan, and J. Nelson, "Hybrid polymer–metal oxide thin films for photovoltaic applications," *J. Mater. Chem.*, vol. 17, pp. 3141–3153, 2007.

[5] B. Sun, H. J. Snaith, A. S. Dhoot, S. Westenhoff, and N. C. Greenham, "Vertically segregated hybrid blends for photovoltaic devices with improved efficiency," *J. Appl. Phys.*, vol. 97, pp. 014914-1–014914-6, 2005.

[6] S. A. McDonald, G. Konstantatos, S. Zhang, P. W. Cyr, E. J. D. Klem, L. Levina, and E. H. Sargent, "Solution-processed PbS quantum dot infrared photodetectors and photovoltaics," *Nat. Mater.*, vol. 4, pp. 138–142, 2005.

[7] K. M. Coakley and M. D. McGehee, "Photovoltaic cells made from conjugated polymers infiltrated into mesoporous titania," *Appl. Phys. Lett.*, vol. 83, pp. 3380–3382, 2003.

[8] C. H. Chang, T. K. Huang, Y. T. Lin, Y. Y. Lin, C. W. Chen, T. H. Chu, and W. F. Su, "Improved charge separation and transport efficiency in poly(3-hexylthiophene)–TiO$_2$ nanorod bulk heterojunction solar cells," *J. Mater. Chem.*, vol. 18, pp. 2201–2207, 2008.

[9] P. Ravirajan, S. A. Haque, J. R. Durrant, D. D. C. Bradley, and J. Nelson, "The effect of polymer optoelectronic properties on the performance of multilayer hybrid polymer/TiO$_2$ solar cells," *Adv. Funct. Mater.*, vol. 15, pp. 609–618, 2005.

[10] J. Bouclé, S. Chyla, M. S. P. Shaffer, J. R. Durrant, D. D. C. Bradley, and J. Nelson, "Hybrid solar cells from a blend of poly (3-hexylthiophene) and ligand-capped TiO$_2$ nanorods," *Adv. Funct. Mater.*, vol. 16, pp. 622–633, 2008.

[11] C. Y. Kwong, W. C. H. Choy, A. B. Djurisic, P. C. Chui, K. W. Cheng, and W. K. Chan, "Poly (3-hexylthiophene):TiO$_2$ nanocomposites for solar cell applications," *Nanotechnology*, vol. 15, pp. 1156–1161, 2004.

[12] W. J. E. Beek, M. M. Wienk, and R. A. J. Janssen, "Efficient hybrid solar cells from zinc oxide nanoparticles and a conjugated polymer," *Adv. Mater.*, vol. 16, pp. 1009–1013, 2004.

[13] P. D. Cozzoli, A. Kornowski, and H. Weller, "Low-temperature synthesis of soluble and processable organic-capped anatase TiO$_2$ nanorods," *J. Amer. Chem. Soc.*, vol. 125, pp. 14539–14548, 2003.

[14] T. W. Zeng, Y. Y. Lin, H. H. Lo, C. W. Chen, C. H. Chen, S. C. Liou, H. Y. Hunag, and W. F. Su, "A large interconnecting network within hybrid MEH-PPV/TiO$_2$ nanorod photovoltaic devices," *Nanotechnology*, vol. 15, pp. 5387–5392, 2006.

[15] J. Y. Kim, S. H. Kim, H. H. Lee, K. Lee, W. Ma, X. Gong, and A. Heeger, "New architecture for high-efficiency polymer photovoltaic cells using solution-based titaniumoxide as an optical spacer," *Adv. Mater.*, vol. 18, pp. 572–576, 2006.

[16] Y. Y. Lin, T. H. Chu, S. S. Li, C. H. Chuang, C. H. Chang, W. F. Su, C. P. Chang, M. W. Chu, and C. W. Chen, "Interfacial nanostructuring on the performance of polymer/TiO$_2$ nanorod bulk heterojunction solar cells," *J. Amer. Chem. Soc.*, vol. 131, pp. 3644–3649, 2009.

[17] Y. Y. Lin, C. W. Chen, T. H. Chu, W. F. Su, C. C. Lin, C. H. Ku, J. J. Wu, and C. H. Chen, "Nanostructured metal oxide/conjugated polymer hybrid solar cells by low temperature solution processes," *J. Mater. Chem.*, vol. 17, pp. 4571–4576, 2007.

[18] Y. Y. Lin, Y. Y. Lee, L. W. Chang, J. J. Wu, and C. W. Chen, "The influence of interface modifier on the performance of nanostructured ZnO/polymer hybrid solar cells," *Appl. Phys. Lett.*, vol. 94, pp. 063308-1–063308-3, 2009.

[19] K. Hara, T. Horiguchi, T. Kinoshita, K. Sayama, H. Sugihara, and H. Arakawa, "Highly efficient photon-to-electron conversion with mercurochrome-sensitized nanoporous oxide semiconductor solar cells," *Solar Energy Mater. Solar Cells*, vol. 64, pp. 115–134, 2000.

[20] R. H. Friend, G. J. Denton, J. J. M. Halls, N. T. Harrison, A. B. Holmes, A. Kohler, A. Lux, S. C. Moratti, K. Pichler, N. Tessler, K. Towns, and H. F. Wittmann, "Electronic excitations in luminescent conjugated polymers," *Solid State Commun.*, vol. 102, pp. 249–258, 1997.

Shao-Sian Li received the B.S. degree in materials science and engineering from National Chiao Tung University, Hsinchu, Taiwan, in 2004, and the M.S. degree in materials science and engineering, in 2006 from National Taiwan University, Taipei, Taiwan, where he is currently working toward the Ph.D. degree in Nano-Materials and Devices Laboratory, Department of Materials Science and Engineering led by Prof. C.-W. Chen.

His research interests include the carrier transport behaviors in polymer/inorganic hybrid materials. He has been engaged in research on correlation between structure and transport properties in nanostructures and bulk heterojunctions based on polymer/metal oxide hybrid materials and also in the carrier dynamics such as recombination at polymer/inorganic interfaces.

Yun-Yue Lin received his B.S. degree in mechanical engineering from National Taiwan University of Science and Technology, Taipei, Taiwan, in 2003, and the M.S. and Ph.D. degrees in materials science and engineering, in 2005 and 2009, respectively, from National Taiwan University, Taipei, Taiwan.

He was in Nano-Materials and Devices Laboratory, Department of Materials Science and Engineering, National Taiwan University, led by Prof. C.-W. Chen. His research has been concerned with the solution processible polymer/inorganic nanomaterials hybrid solar cells in which he had manipulated the nanomorphology of hybrid materials and correlated to the solar cell's performance through electrical, optical, and surface potential studies. He has also been engaged in the development and applications for carbon based materials.

Wei-Fang Su received the Ph.D. degree in polymer chemistry from the University of Massachusetts, Amherst, in 1978.

She was a Postdoctoral Research Fellow at Northwestern University, Evanston, IL, for one year, where she was involved in research on dielectric properties of epoxy resins. Then, she joined Westinghouse Research Center as a Senior Scientist and became a Fellow Scientist after 7 years. During the 16 years tenure at Westinghouse, she was engaged in various projects related to materials for electric insulations and electronic devices. She was a Visiting Scholar in the Materials and Devices Laboratory, Mitsubishi Electric Company, where she was engaged in nonlinear optical materials. Since 1996, she has been a Full Professor in the Department of Materials Science and Engineering, National Taiwan University, Taipei, Taiwan. Her research interests include the innovative materials including liquid crystalline nanocomposite, solventless high refractive index organic–inorganic hybrid material, polymer-nanoparticle hybrid material for LEDs and solar cells. She has authored or coauthored 331 research papers published in various scientific journals and conference proceedings, one book, chapters for six books, and holds 17 U.S. Patents and 9 Taiwan Patents.

Dr. Su is a recipient of six Outstanding Researcher Awards during her tenure with the Westinghouse. She was awarded National Science Council of Taiwan Research Award twice and as a 2003 Chair of Nanotechnology of Far Eastern Y. Z. Hsu Science and Technology Memorial Foundation, and 2008 4th outstanding Nanotechnology Award by Ministry of Economic Affairs of Taiwan.

Chun-Wei Chen received the B.S. degree in electrical engineering from National Taiwan University, Taipei, Taiwan, in 1993, the M.Phil. degree from Cavendish Laboratory, Department of Physics, in 1995, and the Ph.D. degree from Engineering Department, in 1998, both from Cambridge University, Cambridge, U.K.

He joined the faculty of the Department of Materials science and engineering, National Taiwan University in 2002, where he is currently a Professor. His current research interests include the development of low-cost, solution processible solar cells based on polymer/metal oxide hybrid materials, photogenerated carrier dynamics at organic/inorganic interfaces, and the fundamental optoelectronic properties of low-dimensional materials such as carbon nanotube, graphene, and ZnO-related materials.